

Thermally Induced Conversion of Sr-Exchanged LTA- and FAU-Framework Zeolites. Syntheses, Characterization, and Polymorphism of Ordered and Disordered $\text{Sr}_{1-x}\text{Al}_{2-2x}\text{Si}_{2+2x}\text{O}_8$ ($x = 0; 0.15$), Diphyllsilicate, and Feldspar Phases

Radovan Dimitrijević* and Aleksandar Kremenović

Faculty of Mining and Geology, Department of Crystallography, University of Belgrade, Djušina 7, 11000 Belgrade, Yugoslavia

Vera Dondur

Faculty of Physical Chemistry, University of Belgrade, P.O. Box 550, Akademski Trg 16, 11000 Belgrade, Yugoslavia

Magdalena Tomašević-Čanović

Institute for Technology of Nuclear and Other Raw Minerals, France d'Eperea 86, 11000 Belgrade, Yugoslavia

Miće Mitrović

Faculty of Physics, University of Belgrade, P.O. Box 368, Akademski Trg 16, 11001 Belgrade, Yugoslavia

Received: September 19, 1996; In Final Form: December 28, 1996[⊗]

The thermal behavior of fully Sr-exchanged LTA- and FAU-framework zeolites was followed in the temperature range from ambient to 1500 °C. Both zeolite frameworks collapsed into amorphous intermediate substances after heating between 780 and 950 °C. Prolonged annealing of these products above 950 °C induces their recrystallization to ordered hexagonal $\text{SrAl}_2\text{Si}_2\text{O}_8$, [$a_0 = 5.1970(2)$ Å, $c_0 = 15.200(1)$ Å] and disordered hexagonal $\text{Sr}_{0.85}\square_{0.15}\text{Al}_{1.71}\text{Si}_{2.29}\text{O}_8$ [$a_0 = 5.2039(2)$ Å, $c_0 = 15.158(1)$ Å], diphyllsilicate phases, respectively. These phases are unstable under prolonged heating, and near 1100 °C, they can be polymorphously transformed into corresponding Sr-feldspar_{LTA} [$a_0 = 8.358(2)$ Å, $b_0 = 12.941(3)$ Å, $c_0 = 7.114(1)$ Å, $\beta = 115.26(2)^\circ$] and Sr-feldspar_{FAU} [$a_0 = 8.354(2)$ Å, $b_0 = 12.957(3)$ Å, $c_0 = 7.128(2)$ Å, $\beta = 115.27(2)^\circ$] phases, maintaining framework cation-ordering characteristics. The phase conversions in the temperature range investigated were followed by thermal (DTA, TGA, and DSC), XRPD, and SEM analyses. The structural mechanism for $\text{M}_{1-x}\text{Al}_{2-2x}\text{Si}_{2+2x}\text{O}_8$ ($\text{M} = \text{Ca}, \text{Sr}, \text{Ba}, \text{Pb}$) polymorphous transformation from diphyllsilicate to feldspar topology is discussed.

I. Introduction

Due to a range of convenient thermomechanical, electrical, and other properties, the alkaline earth aluminosilicates having framework topologies such as hexacelsian, celsian, cordierite, and anorthite are very interesting materials. Recently published results^{1–5} on these and other aluminosilicate ceramics, pointed to synthetic cation-exchanged LTA-, FAU-, ABW-, and GIS⁶-framework zeolites as good precursors for their syntheses. All these ceramics were obtained in the processes of thermally induced phase transformations of synthetic zeolites, whereas the procedure has been proposed as a method⁷ for designing electronic ceramics. Meanwhile, by a zeolite conversion route several new aluminosilicate compounds such as Ag-carnegieite,⁸ γ -eucryptite,^{9,10} δ -eucryptite,¹¹ and CsAlSiO_4 with the ANA-framework¹² topology have been synthesized. Therefore, the discussed synthesis route has been proposed as a method for obtaining new aluminosilicate and oxide materials as well.

Thermally induced structural conversion of synthetic cation-exchanged zeolites into the other crystalline phases is preceded by formation of an intermediate amorphous substance. The type and valence state of extraframework cations give rise to recrystallization of amorphous substances to different framework topologies. Some of synthesized aluminosilicate phases that

occurred among the thermally induced products are otherwise difficult or impossible to obtain by classical syntheses. Accordingly, the discussed method of synthesis could be considered as a novel route for the investigation of three-component $\text{MO}-\text{Al}_2\text{O}_3-\text{SiO}_2$ ($\text{M} = \text{monovalent or divalent cation}$) phase systems as well.

The work presented here continues previous studies^{1–3} on thermally induced structural conversions of LTA-, FAU-, and GIS-framework zeolites exchanged with alkaline earth metals and syntheses of $\text{MAl}_2\text{Si}_2\text{O}_8$ ($\text{M} = \text{Ca}, \text{Sr}, \text{Ba}, \text{Pb}$) aluminosilicate ceramics. Our interest is focused on the $\text{SrO}-\text{Al}_2\text{O}_3-\text{SiO}_2$ phase system, i.e. syntheses and characterization of the stoichiometric and nonstoichiometric Sr-diphyllsilicate^{2,13} and Sr-feldspar¹⁴ phases.

II. Experimental Section

Sodium zeolites with LTA (type A; $\text{Si}/\text{Al} = 1.00$) and FAU (type X; $\text{Si}/\text{Al} = 1.34$) framework, manufactured by Union Carbide Co., were used as starting materials. Fully exchanged Sr^{2+} forms of these zeolites were prepared after several successive exchanges from concentrated SrCl_2 solutions.

The chemical composition of the samples was analyzed by atomic absorption spectrophotometry, using a Perkin Elmer 380 instrumental device.

[⊗] Abstract published in *Advance ACS Abstracts*, April 15, 1997.

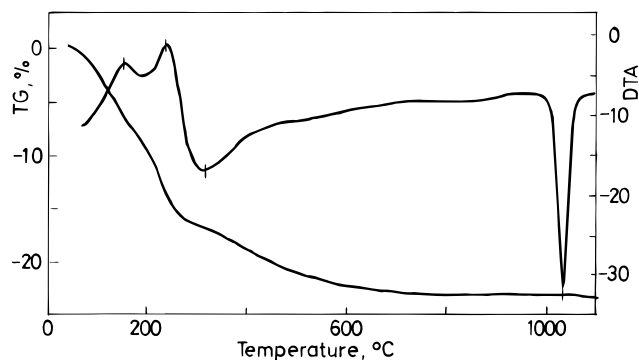


Figure 1. Thermal (DTA and TGA) curves of initial Sr-exchanged LTA-framework zeolite.

The thermal behavior (DTA, TGA, and DSC) of zeolites and synthesized Sr-diphylosilicate phases was investigated using a Netzsch simultaneous analyzer, model STA-409 EP, equipped with high-temperature DSC (1200 °C) and DTA cells. Both starting zeolite precursors were examined at a heating rate of 10°/min. Phase composition was analyzed by the X-ray powder diffraction (XRPD) method. A Netzsch-421 type furnace was used for heating the samples at temperatures over 1100–1500 °C. The samples were annealed at different temperatures for 1 h. All XRPD experiments were performed after cooling.

The XRPD patterns were obtained on a Philips, PW-1710 automated diffractometer, using a Cu tube operated at 40 kV and 35 mA. The instrument was equipped with the diffracted beam curved graphite monochromator and a Xe-filled proportional counter. Diffraction data were collected in the 2θ range, 4–70°, counting for 0.25 and 2.50 s at 0.02 steps. Fixed 1° divergence and 0.1° receiving slits were used. The least-squares program Lsucip¹⁵ was used for the refinement of cell dimensions from the powder data.

Investigations of crystal morphology of synthesized phases were carried out with scanning electron microscopy, using a JEOL 840A instrument. The samples investigated were gold sputtered in a JFC 1100 ion sputterer.

III. Results

The results of thermal analysis (DTA and TGA) of fully Sr-exchanged LTA-framework zeolite, obtained in the range from ambient temperature to 1100 °C, are shown in Figure 1. Two endothermic peaks at 152 and 238 °C correspond to the loss of zeolitic water. A weak, broadened exothermic peak and very strong ones are noticed at 315 and 1031 °C, respectively. From the TG curve, Figure 1, it is obvious that the dehydration process is intense in the temperature range up to 400 °C, but it has been prolonged and finished at nearly 700 °C, corresponding to a 23.5% weight loss.

In Figure 2, the thermal analysis results of fully Sr-exchanged FAU-framework zeolites are shown. The DTA curve is characterized by the occurrence of a broad asymmetric endothermic peak at 203 °C, connected to loss of zeolitic water. Dehydration is completed at 600 °C, corresponding to a 25.6% weight loss. Another characteristic of the DTA curve, Figure 2, is the occurrence of two well-formed strong exothermic peaks at 953 and 1050 °C, respectively.

The XRPD investigations of Sr-exchanged LTA- and FAU-framework zeolite phase conversions, in the temperature range from ambient up to 1100 °C, were carried out on the samples chosen with reference to the results of the thermal measurements presented in Figures 1 and 2. It is clear from Figures 3a,b and 4a,b that initial Sr-zeolite precursors, after dehydration, collapse into corresponding amorphous intermediate products. These

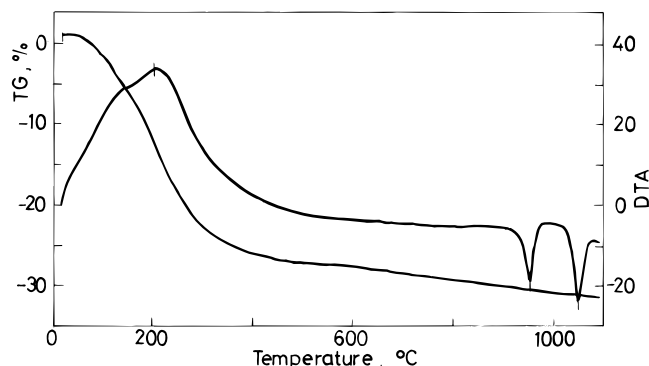


Figure 2. Thermal (DTA and TGA) curves of initial Sr-exchanged FAU-framework zeolite.

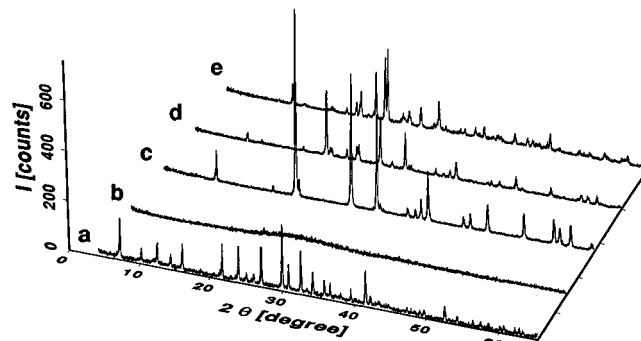


Figure 3. XRPD patterns of (a) initial Sr-exchanged LTA-framework zeolite, 25 °C; (b) amorphous intermediate substance, 900 °C, 1 h; (c) pure stoichiometric hexagonal Sr-diphylosilicate_{LTA} phase, 990 °C, 1 h; (d) mixture of Sr-diphylosilicate_{LTA} and Sr-feldspar_{LTA} phases, 1150 °C, 1 h; (e) pure stoichiometric monoclinic Sr-feldspar_{LTA} phase, obtained at 1300 °C for 1 h.

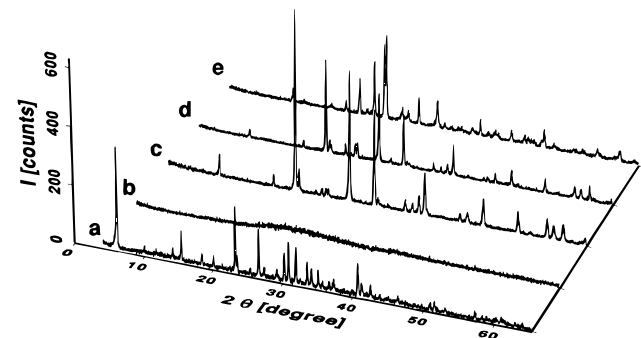


Figure 4. XRPD patterns of (a) initial Sr-exchanged FAU-framework zeolite, 25 °C; (b) amorphous intermediate substance, 900 °C, 1 h; (c) pure nonstoichiometric hexagonal Sr-diphylosilicate_{FAU} phase, 990 °C, 1 h; (d) mixture of Sr-diphylosilicate_{FAU} and Sr-feldspar_{FAU} phases, 1100 °C, 1 h; (e) pure nonstoichiometric monoclinic Sr-feldspar_{FAU} phase, obtained at 1300 °C for 1 h.

TABLE 1: Unit Cell Dimensions of Stoichiometric and Nonstoichiometric Phases Synthesized from Sr-Exchanged LTA- and FAU-Framework Zeolites Respectively

compound	a_0 (Å)	b_0 (Å)	c_0 (Å)	β_0 (°)	γ (°)
Sr-diphylosilicate _{LTA}	5.1970(2)	5.1970(2)	15.200(1)	120.00	
Sr-diphylosilicate _{FAU}	5.2039(2)	5.2039(2)	15.158(1)	120.00	
Sr-feldspar _{LTA}	8.358(2)	12.941(3)	7.114(1)	115.26(2)	
Sr-feldspar _{FAU}	8.354(2)	12.957(3)	7.128(2)	115.27(2)	

substances formed at 900 °C were used as the starting materials for further high-temperature investigations, respectively. With prolonged heating the amorphous products start to recrystallize into Sr-diphylosilicate phases^{2,13} (Figures 3c and 4c), which are stable up to nearly 1100 °C. Both phases were investigated by the DSC method in the range from ambient temperature up

TABLE 2: Chemical Analyses (% wt) and Crystallochemical Formulas of Phases Synthesized from Sr-Exchanged LTA- and FAU-Framework Zeolites as Initial Materials

compound	SiO ₂	Al ₂ O ₃	SrO	Na ₂ O	Σ (%)	crystallochemical formula
dehydrated ^a Sr-exchanged LTA-framework zeolite	36.90	31.37	31.89	0.07	100.23	(Sr _{6.00} Na _{0.04}) _{6.04} [Al _{11.98} Si _{12.01}] _{23.99} O ₄₈
dehydrated Sr-exchanged FAU-framework zeolite	43.88	27.83	28.14	0.24	100.09	(Sr _{40.82} Na _{1.17}) _{41.99} [Al _{82.04} Si _{109.77}] _{191.81} O ₃₈₄
Sr-diphyllsilicate _{LTA}	36.91	31.27	31.87		100.05	SrAl ₂ Si ₂ O ₈
Sr-feldspar _{LTA}						
Sr-diphyllsilicate _{FAU}	43.98	27.81	28.32		100.11	Sr _{0.85} □ _{0.15} Al _{1.71} Si _{2.29} O ₈
Sr-feldspar _{FAU}						

^a The water contents of hydrated Sr-exchanged LTA- and FAU-framework zeolites are determined from TGA analyses as 23.5% and 25.6%, respectively.

to 900 °C. A weak endothermic peak corresponding to the hexagonal–orthorhombic^{16,17} transition is detected at 765 °C for the Sr-diphyllsilicate phase synthesized from Sr-exchanged LTA-framework zeolite, whereas in the case of Sr-exchanged FAU-framework zeolite precursor, this transition was not observed.

On further annealing over 1100 °C, synthesized Sr-diphyllsilicate phases started solid–solid polymorphous transformations into the corresponding Sr-feldspar phases (Figures 3d and 4d), which are accomplished at 1300 °C (Figure 3e and 4e). Both synthesized Sr-feldspars are stable at 1500 °C. The XRPD patterns of the products originated from the initial Sr-zeolites, (Figures 3 and 4) were indexed and compared with JCPDS data (card files 35–73 and 38–1454, respectively). The calculated unit cell dimensions are presented in Table 1, whereas tables containing indexed powder patterns as supporting information submitted to JCPDS (see paragraph at the end of this article).

Chemical composition of synthesized Sr-diphyllsilicate and Sr-feldspar phases, as well Sr-zeolites, Table 2, shows that complete Sr²⁺ → Na⁺ exchange on initial zeolites was achieved. From these analyses, crystallochemical formulas for phases synthesized were calculated on the basis of eight oxygen atoms. It follows that phases originated from Sr-exchanged LTA-framework zeolites are stoichiometric, whereas those obtained from Sr-exchanged zeolites FAU-framework are nonstoichiometric. Accordingly, these topologically identical but chemically different phases would be ascribed with subscript LTA or FAU, for practical distinction, as it was stated in Tables 1 and 2.

In Figure 5, a SEM images evolution on calcination Sr-exchanged LTA-framework and FAU-framework zeolite is shown. Observed initial zeolites with developed cubic crystal forms are presented in parts a and e of figure 5, respectively. A predominately rounded grain form, observed in Figure 5b, f, shows that sintering processes at 940 °C are spread. At 1050 °C, this processes proceeded in the formation of grains having lamellar texture (Figure 5c,g), characteristic for diphyllsilicate compounds. Finally, after prolonged heating at 1500 °C, the lamellar grain texture is preserved, Figure 5d, h.

IV. Discussion

Thermal Conversion of Zeolites as a New Method For Investigation of Aluminosilicate Phase Systems. Very few systematic studies have been made on synthesis of Sr-aluminosilicates from the SrO–Al₂O₃–SiO₂ phase system. Syntheses of SrAl₂Si₂O₈ phases isomorphous to monoclinic and hexagonal celsian were established by Sorrel,¹⁸ from the clay and Sr-sulfate mixture in the sintering reaction at 1400 °C. The reactions in a similar system, kaolinite–strontium oxide, under hydrothermal conditions was investigated by Schytova.¹⁹ Those results obtained on hydrothermal crystallization of Sr-aluminosilicate gels, made by Barrer,²⁰ are the most systematic ones. Syntheses of stoichiometric and nonstoichiometric SrAl₂Si₂O₈ phases, following Sr-feldspar^{21–24} crystallochemistry, were prepared by

solid state reactions of oxide mixtures at high temperatures or dry crystallization from the melt and glasses with corresponding compositions. The role of Sr²⁺-cations in the densification mechanism of Sr-zeolite-A to the low-dielectric ceramic Sr-Anorthite have been investigated by Parise²⁵ as well.

The described zeolite thermal conversion route could be considered as a new method for synthesis of Sr-aluminosilicates in the SrO–Al₂O₃–SiO₂ phase system. Synthesized Sr-diphyllsilicate_{LTA} and Sr-feldspar_{LTA} compounds, obtained from Sr-exchanged LTA-framework zeolites as initial material, are situated on the SrAl₂O₃–SiO₂ join. High-silica counterpart phases prepared from Sr-exchanged FAU-framework zeolites as another initial material are located beside the mentioned join in the field of siliceous composition, according to a higher Si/Al = 1.34 ratio, Table 2. The crystal lattices of stoichiometric (Sr-diphyllsilicate_{LTA} and Sr-feldspar_{LTA}) and nonstoichiometric (Sr-diphyllsilicate_{FAU} and Sr-feldspar_{FAU}) counterpart phases are very sensitive to changes of Si/Al ratios which could be followed by measuring the unit cell dimensions, Table 1.

In the case of hexagonal Sr-diphyllsilicate phases, changes along the *c*₀ axis are expressive. The shrinkage of the nonstoichiometric hexagonal Sr_{0.85}□_{0.15}Al_{1.71}Si_{2.29}O₈ phase of 0.3% along the *c*₀ axis, in relation to the stoichiometric hexagonal SrAl₂Si₂O₈ phase, is directly influenced by the increase of shorter Si–O–Si bridging bonds in the double-tetrahedra^{2,3} layers. Similar contraction values were observed at isostructural hexacelsian¹ phase obtained by the same syntheses route. It is clear that changes of Si/Al ratios in the double-tetra-layered framework create the vacant (□) extraframework cation sites on its surface.

The crystal lattices of the Sr-feldspar phases obtained as a product of prolonged heating of corresponding Sr-diphyllsilicate phases are sensitive to Si/Al ratio changes as well. In our experiments, the differences between Sr-feldspar_{LTA} and Sr-feldspar_{FAU} samples are visible along the *b*₀ and *c*₀ axes, but according to structural investigations,^{21–23} the *a*₀ axis is most sensitive to changes of Si/Al ratio, Table 1. In our opinion, these differences arise as a consequence of complex order–disorder phenomena (Sr-vacancies and T-cations) which could involve the preparation route.

Results presented here on the synthesis of Sr-diphyllsilicate and Sr-feldspar phases, compared to classical ceramic preparation, clearly shows advantages of the zeolite conversion route. By this method, the aforementioned Sr-aluminosilicates and other ceramics such as hexacelsian,¹ anorthite,³ or β-eucryptite^{9,10} could be prepared for 1 h at appropriate temperatures, a rapidly reduced synthesis procedure. Moreover, thermally induced zeolite conversion synthesis methods enable production of ceramic compounds having a proposed stoichiometry that is shown in the case of the investigated Sr-aluminosilicate phases.

Structural Mechanism of Sr-Diphyllsilicate to Sr-Feldspar Polymorphous Transformation. From the results of thermal conversion of Sr-exchanged LTA- and FAU-framework zeolites in the temperature range investigated, it is clear that

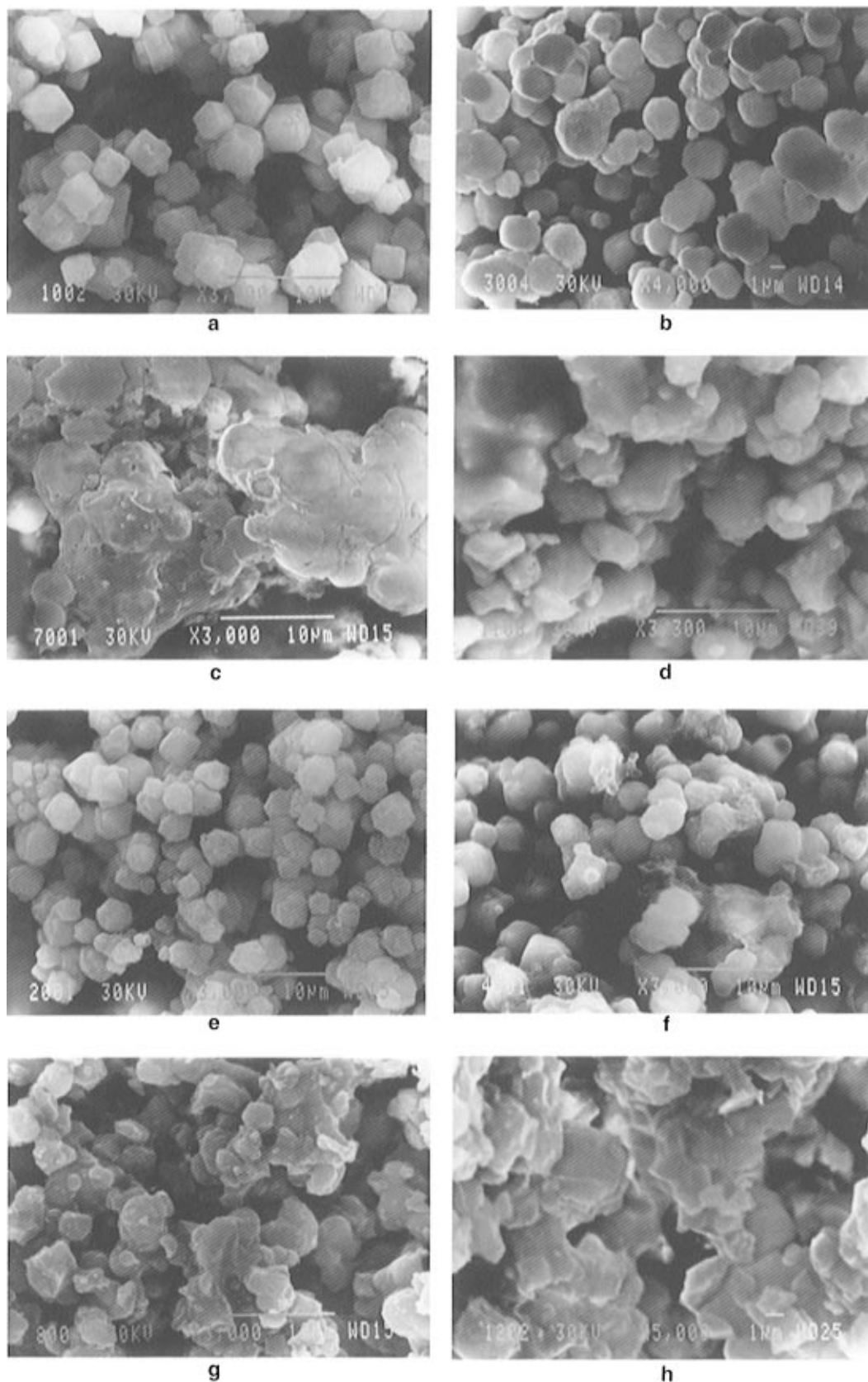


Figure 5. Scanning electron microphotographs of initial Sr-exchanged LTA- and FAU-framework zeolites (a and e) heated at different temperatures: 940 °C (b and f), 1050 °C (c and g), and 1500 °C (d and h), respectively.

the final outcome is the Sr-feldspars, Figures 3e and 4e. Similar conversion routes, as well as topotactic transition of diphylosilicate to feldspar topology, are observed in the cases of Ca-exchanged LTA,³ Sr-exchanged LTA,²⁵ Ba-exchanged GIS, Pb-exchanged LTA, and Pb-exchanged FAU²⁶ species. Therefore, it is of crystallochemical interest to consider the whole mech-

anism of transformation, since the initial zeolites and synthesized diphylosilicate and feldspar framework topologies differ considerably.

The process of thermally induced structural conversion of zeolites can be roughly schematized³ into three steps. The first stage, corresponding to the dehydration processes and rear-

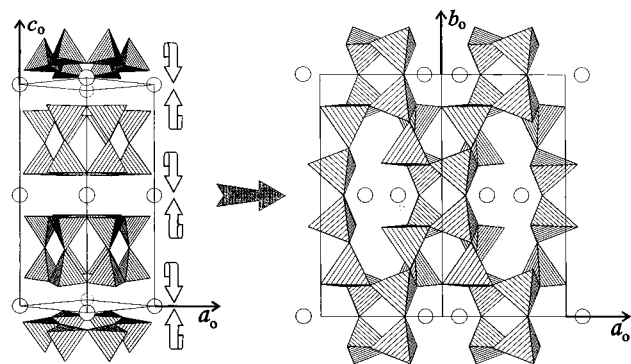


Figure 6. Schematic view of thermally induced polymorphous conversion mechanism of (a) Sr-diphyllsilicate topology to (b) Sr-feldspar framework topology. The crystal structure projections³¹ are given normal to the c_0 and b_0 axes, respectively. The arrows show possible rotations of some tetrahedra from diphyllsilicate (2D) layers and simultaneous binding to feldspar (3D) framework.

range²⁷ of extraframework cations, finally proceeds in breaking of tetrahedral T—O—T bridges with simultaneous collapse of zeolite structure. From the thermal curves and XRPD patterns obtained, Figures 1–4, it is obvious that observed dehydration processes at Sr-exchanged LTA- and FAU-framework zeolites are mutually distinct. The second stage involves the processes of structural reorganization²⁸ of (Si,Al) O_4 tetrahedra and/or secondary building units⁶ that occur in the amorphous intermediate product. The differences observed in the DTA results pointed to specific features of the investigated amorphous²⁶ Sr-precursors, as well as the recrystallization mechanism to Sr-diphyllsilicate phases.

The final stage of thermal conversion includes the polymorphous transformations to the more stable crystalline phase. As it was stated earlier, such polymorphous transitions are observed at all known $MA_2Si_2O_8$ diphyllsilicate phases, including synthesized hexagonal $SrAl_2Si_2O_8$ and $Sr_{0.85}\square_{0.15}Al_{1.71}Si_{2.29}O_{8.00}$ phases. Therefore, it is interesting to discuss the polymorphous conversion Sr-diphyllsilicate \rightarrow Sr-feldspar topology from structural aspects, which are enlightened by knowledge of Sr-diphyllsilicate² and Sr-feldspar^{14,21,22} crystal structures.

The Sr-diphyllsilicate structure² is composed of infinite double-tetrahedra layers, Figure 6a, where double-crankshaft (cc), as well as zigzag (zz), tetrahedra chains²⁹ could be recognized. It is obvious from this figure that the system of double-crankshaft tetrahedra chains, parallel to a_0 and b_0 directions, exist. Another feature of diphyllsilicate structure is the specific two-dimensional framework topology of the double-tetrahedra layer, Figure 6a. In the framework described, a secondary building unit⁶ such as S4R and D6R tetrahedra rings could be recognized. In other words, the double aluminosilicate tetrahedra sheets ($Al_{2-2x}Si_{2+2x}O_8$) are mutually separated by layers of Sr^{2+} cations. At stoichiometric Sr-diphyllsilicate_{LTA} phase ($x = 0$), extraframework Sr^{2+} cation sites are fully occupied, whereas at isostructural nonstoichiometric Sr-diphyllsilicate_{FAU} species ($x = 0.15$), the vacant (\square) sites exist.

The double-crankshaft tetrahedra chain (cc) motif, as well as S4R and S6R building units,⁶ are characteristic for the monoclinic stoichiometric²¹ and isostructural nonstoichiometric²² Sr-feldspar structures as well. But it is important to emphasize that the six-member rings in the Sr-feldspar frameworks are generally irregular and nonplanar. These elements of similarity with the corresponding ones in the Sr-diphyllsilicate structures are sufficient for consideration of one simple mechanism of polymorphous conversion.

Our structural results on thermal behavior of the hexagonal $MA_2Si_2O_8$ diphyllsilicate phases^{1–3} show that their stability is strongly dependent on cation size, following the order $Ba^{2+} > Sr^{2+} > Ca^{2+} > Pb^{2+}$. The cations M^{2+} are six-coordinated (trigonal antiprism) to the three nearest O_{II} oxygens from the surfaces of opposite diphyllsilicate layers, Figure 6a. More precisely speaking, the M^{2+} cations are situated on the 6_3 screw axis between the two regular hexagonal prisms (D6R units). In the case of the investigated Sr-diphyllsilicates, each Sr^{2+} cation is surrounded by six others in the Sr^{2+} -layer, so the direction along the 6_3 axis is preferable for thermal vibrations. This is consistent with the local symmetry at 2b sites of the $P6_3/mcm$ (193) space group. Furthermore, the thermal motion of Sr-atoms in the Sr-diphyllsilicate lattices is found to be twice-as-large thermal ellipsoids, elongated in the c -axis direction, which is determined by Rietveld structural² refinement from XRPD data.

Prolonged temperature/time treatment of Sr-diphyllsilicate phase induces the increase of thermal vibrations of Sr^{2+} cations along the 6_3 axis, as well as oxygens on the surface of diphyllsilicate layers. At critical³⁰ temperatures, the thermal vibrations of Sr^{2+} cations result in extreme elongations along the 6_3 axis with its probable penetration inside the empty space of hexagonal prisms (D6R unit). At this moment, due to rapid changes of Sr^{2+} coordination polyhedra, some T— O_{II} —T bridges would be broken. This action induces the rotation of some TO_4 tetrahedra around Sr^{2+} cations in the plane of the diphyllsilicate layer and its simultaneous binding to tetrahedra from neighboring diphyllsilicate layers, Figure 6a. With prolonged temperature/time treatment transformation mechanism acceleration and at the end of the process (ca. 1200 °C), the 3D Sr-feldspar framework is formed; i.e., polymorphous transformation is finished, Figure 6b. The proposed conversion mechanism is simplified, but several facts speak in favor of its reality. Here we want to emphasize the metric identity observed along the c_0 axis at corresponding hexagonal and monoclinic polymorphous pairs, which would be obtained by summing the tetrahedra dimensions. Our interpretation of Sr-diphyllsilicate \rightarrow Sr-feldspar topotactic framework conversion is comparable with those proposed by Parise,²⁵ on the basis of EXAFS measurements.

Supporting Information Available: Tables listing features in the powder X-ray diffraction patterns of the pure stoichiometric $SrAl_2Si_2O_8$ and nonstoichiometric $Sr_{0.85}\square_{0.15}Al_{1.71}Si_{2.29}O_{8.00}$ (Sr-diphyllsilicate and Sr-feldspar) phases have been deposited with JCPDS. For ordering information, contact: International Centre for Diffraction Data, 1601 Park Lane, Swathmore, PA, 19081.

References and Notes

- (1) Dondur, V.; Dimitrijević, R.; Kremenović, A.; Mioč, U.; Srejić, R.; Tomašević, M. In *Advanced Science and Technology 3*; Vincenzini, P., Ed.; Techna: Faenza, 1995; Part 3, pp 687–694.
- (2) Kremenović, A.; Dimitrijević, R.; Dondur, V.; Srejić, R. In *Proceedings of the XV European Crystallographic Meeting*, Dresden, 1995; p 420 (Abstract).
- (3) Dimitrijević, R.; Dondur, V.; Kremenović, A. *Zeolites* **1996**, *16*, 294.
- (4) Berger, A.; Samsonova, T.; Akovlev, I. *Izv. Akad. Nauk. SSSR, Ser. Himičeskaja* **1971**, *10*, 2129.
- (5) Sankar, G.; Wright, P.; Natarajan, S.; Thomas, J.; Neville-Greaves, G.; Dent, A.; Dobson, B.; Ramsdale, C.; Jones, R. *J. Phys. Chem.* **1993**, *97*, 9550.
- (6) Meier, W.; Olson, D. *Atlas of Zeolite Structure Types*; Structure Commission of the IZA, Ed. *Zeolites* **1992**, *12*, 449.
- (7) Corbin, D.; Parise, J.; Chowdry, U.; Subramanian, M. *Mater. Res. Soc. Symp. Proc.* **1991**, *233*, 213.
- (8) Petranović, N.; Dimitrijević, R. *Thermochim. Acta* **1985**, *84*, 227.
- (9) Dondur, V.; Dimitrijević, R. *J. Solid State Chem.* **1986**, *63*, 46.
- (10) Norby, P. *Zeolites* **1990**, *10*, 193.
- (11) Newsam, J. *J. Phys. Chem.* **1988**, *92*, 445.

- (12) Dimitrijević, R.; Dondur, V.; Petranović, N. *J. Solid State Chem.* **1991**, 95, 335.
- (13) Liebau, F. In *Structural Chemistry of Silicates*; Springer: Berlin, 1985.
- (14) Smith, J. In *Feldspar Minerals. I. Crystal Structures and Physical Properties*; Springer: Berlin, 1974.
- (15) Garvey, P. *Powder Diff.* **1986**, 1, 114.
- (16) Topel-Schadt, J.; Muller, W.; Pentinghaus, H. *J. Mater. Sci.* **1978**, 13, 1809.
- (17) Bansal, N.; Hyatt, M.; Drummond, C. *Ceram. Eng. Sci. Proc.* **1991**, 12, 1222.
- (18) Sorrell, C. *Am. Mineral.* **1963**, 47, 291.
- (19) Shytova, V.; Kosorykov, A.; Ovčarenko, F. *Zh. Neorg. Khim.* **1980**, 25, 359.
- (20) Barrer, R.; Marshall, D. *J. Chem. Soc.* **1964**, 485.
- (21) Chiari, G.; Calleri, M.; Bruno, E.; Ribbe, P. *Am. Mineral.* **1975**, 60, 111.
- (22) Grundy, H.; Ito, J. *Am. Mineral.* **1974**, 59, 1319.
- (23) Bambauer, H.; Schops, M.; Pentinghaus, H. *Bull. Mineral.* **1984**, 107, 541.
- (24) Wong, Ng.; McMurdie, H.; Paretzkin, B.; Hubbard, C.; Drago, A. *Powder Diff.* **1987**, 2, 114.
- (25) Parise, J.; Corbin, D.; Subramanian, M. *Mater. Res. Bull.* **1989**, 24, 303.
- (26) Dimitrijević, R.; Kremenović, A.; Dondur, V. To be published.
- (27) Alberti, A.; Vezzallini, G. In *Proceedings of the Sixth International Zeolite Conference*; Olson, D., Bisio, A., Eds.; Butterworths: Guilford, UK, 1984; p 834.
- (28) Kirkpatrick, R. *Am. Mineral.* **1983**, 68, 66.
- (29) Smith, J. *Chem. Rev.* **1988**, 88, 149.
- (30) Bansal, N.; Drummond, C. *J. Am. Ceram. Soc.* **1993**, 76 (5), 1321.
- (31) Fischer, R. *J. Appl. Crystallogr.* **1985**, 18, 258.